Journal of Power Sources 215 (2012) 63–68

Contents lists available at SciVerse ScienceDirect

Journal of Power Sources

journal homepage: www.elsevier.com/locate/jpowsour

Enhanced rate and high-temperature performance of $La_{0.7}Sr_{0.3}MnO_3$-coated $LiNi_{0.5}Mn_{1.5}O_4$ cathode materials for lithium ion battery

Guiying Zhao, Yingbin Lin*, Ting Zhou, Ying Lin, Yandan Huang, Zhigao Huang**

College of Physics and Energy, Fujian Normal University, Fuzhou 350007, China

HIGHLIGHTS

- With $La_{0.7}Sr_{0.3}MnO_3$-coating the rate performance and thermal storage of $LiNi_{0.5}Mn_{1.5}O_4$ is improved.
- High conductive $La_{0.7}Sr_{0.3}MnO_3$ is responsible for the improved performance at high-temperature.
- $La_{0.7}Sr_{0.3}MnO_3$ layer suppresses the Mn dissolution and reduce the charge-transfer resistance.

ARTICLE INFO

Article history:
Received 16 February 2012
Received in revised form
23 April 2012
Accepted 27 April 2012
Available online 3 May 2012

Keywords:
Lithium-ion battery
Cathode
Surface modification
Perovskite

ABSTRACT

$La_{0.7}Sr_{0.3}MnO_3$-coated 5 V spinel $LiNi_{0.5}Mn_{1.5}O_4$ as cathode is prepared by mixing $LiNi_{0.5}Mn_{1.5}O_4$ powders and the sol–gel-drived $La_{0.7}Sr_{0.3}MnO_3$ matrix, followed by high-temperature calcinations. The effect of $La_{0.7}Sr_{0.3}MnO_3$-coating on the electrochemical performances of $LiNi_{0.5}Mn_{1.5}O_4$ cells, especially at elevated temperature, is investigated systematically by the charge/discharge testing, cyclic voltammograms and AC impedance spectroscopy, respectively. Compared to pristine $LiNi_{0.5}Mn_{1.5}O_4$, $La_{0.7}Sr_{0.3}MnO_3$-coated material has much lower surface and charge-transfer resistances and shows a higher lithium diffusion rate. The results of electrochemical experiments demonstrate that the modified material exhibits remarkably enhanced electrochemical reversibility and stability at elevated temperature. The $La_{0.7}Sr_{0.3}MnO_3$-coating layer protected the surface of the active materials from HF in the electrolyte during electrochemical cycling. As a result, the electrochemical cycling stability is improved.

1. Introduction

During past few years, spinel $LiNi_{0.5}Mn_{1.5}O_4$ and variants as cathode material have been attracted much intensive interest due to its high discharge capacity and attractive voltage plateau at around 4.7 V, which leads to their potential application in electric vehicle and plug-in hybrid electric vehicle [1–3]. Although considerable progress has been made in spinel cathodes as far, capacity fading on cycling unavoidably occurs due to Mn dissolution from spinel particles in the presence of HF in electrolyte, especially at elevated temperature or high voltage [4,5]. Significant efforts have made to improve cyclability of spinel $LiNi_{0.5}Mn_{1.5}O_4$ and the surface modification is well-known as an effective way in reducing the rate of Mn dissolution into electrolyte [6–9]. For instance, Fan et al. [6] have found that the surface modification of $LiNi_{0.5}Mn_{1.5}O_4$ with SiO_2 demonstrates obviously improved capacity retention rate. Shi et al. [7] have reported that surface modified $LiNi_{0.5}Mn_{1.5}O_4$ by $AlPO_4$ exhibits dramatically enhanced electrochemical reversibility and stability at elevated temperature. In contrast, $La_{0.7}Sr_{0.3}MnO_3$ with high electronic conductivity (over 100 S cm^{-1}) [10] seems to be more promising as a coating material since conductive coating can enhance the surface intercalation reaction of lithium ions, reduce cell polarization and inter-particle resistance and contact between active electrode materials and electrolyte solution [11,12]. Guo et al. [13] reported that $LiFePO_4$ cathodes coated with $La_{0.7}Sr_{0.3}MnO_3$ demonstrate excellent electrochemical performance at high rate charge/discharge. Based on this idea, the surface modification of $LiNi_{0.5}Mn_{1.5}O_4$ with $La_{0.7}Sr_{0.3}MnO_3$ was synthesized and the thermal stability and electrochemical performance at elevated temperature of composites were systematically investigated.

2. Experimental

2.1. Preparation and characterization of cathode materials

$LiNi_{0.5}Mn_{1.5}O_4$ and $LiNi_{0.5}Mn_{1.5}O_4$ coated with $La_{0.7}Sr_{0.3}MnO_3$ composites were fabricated by a sol–gel thermolysis process.

* Corresponding author. Tel./fax: +86 591 2286 8132.
** Corresponding author. Tel./fax: +86 591 2286 7577.
E-mail addresses: yblin@fjnu.edu.cn (Y. Lin), zghuang@fjnu.edu.cn (Z. Huang).

0378-7753/$ – see front matter © 2012 Elsevier B.V. All rights reserved.
doi:10.1016/j.jpowsour.2012.04.090

Analytical grade $LiCH_3COO{\cdot}2H_2O$, $Mn(CH_3COO)_2{\cdot}6H_2O$, and $Ni(CH_3COO)_2{\cdot}4H_2O$ in stoichiometric amounts were dissolved in de-ionized water containing proper amount of citric acid solution followed by stirring at 80 °C until the polymerized gel was formed. The obtained gel is dried at 120 °C for 24 h, resulting in the formation of amorphous powders. The powder was further sintered at 500 °C for 12 h to complete organic removal and subsequently calcined at 900 °C for 12 h to obtain final products of $LiNi_{0.5}Mn_{1.5}O_4$. $(LiNi_{0.5}Mn_{1.5}O_4)_{94}/(La_{0.7}Sr_{0.3}MnO_3)_6$ cathode material was prepared by mixing appropriate amounts of obtained $LiNi_{0.5}Mn_{1.5}O_4$ powder with $La_{0.7}Sr_{0.3}MnO_3$ gel under ultrasonic-treatment for 10 h, where the preparation of $La_{0.7}Sr_{0.3}MnO_3$ gel was described in detail in our previous work [14]. The resulted gel is dried at 120 °C in atmosphere, followed by calcinations at 900 °C for 12 h to obtain the final products. The crystal structures of the samples in powder configuration were characterized with a Rigaku MiniFlex II diffractometer with CuK_α radiation (λ = 0.15405 nm). The microstructure and morphology of sintered powder were detected at room temperature by scanning electron microscopy (SEM, JSM-7500F, Japan). The dissolved amounts of transition metal elements were analyzed by inductively coupled plasma OES spectrometer (ICP, Ultima 2, Jobin Yvon).

2.2. Cell fabrication and characterization

Cathodes for electrochemical tests were prepared by homogeneously pasting a slurry containing 80 wt.% active material ($LiNi_{0.5}Mn_{1.5}O_4$ or $(LiNi_{0.5}Mn_{1.5}O_4)_{94}/(La_{0.7}Sr_{0.3}MnO_3)_6$), 10 wt.% super-P and 10 wt.% polyvinylidene fluoride (PVDF) dissolved in *N*-methyl-2-pyrrolidone onto an Al foil and dried in a vacuum at 110 °C over night. The coin cells (R2025) were assembled in an argon-filled glove box (Mikrouna, Super 1220/750, China) with Li metal lithium as a counter electrode, Celgard 2300 microporous polyethylene membrane as the separator and 1 M $LiPF_6$ in a mixture of ethyl carbonate (EC) and dimethyl carbonate (DMC) (1:1 in vol. ratio) as the electrolyte. Galvanostatic charge/discharge measurements were carried out in the voltage range of 3.0–4.9 V with a CT2001A cell test instrument (LAND Electronic Co.). Formation of a stable solid electrolyte interphase (SEI) layer on the spinel cathode surface is responsible for obtained stable cycling ability. To form SEI layer on the spinel cathode surface and highlight the positive role of $La_{0.7}Sr_{0.3}MnO_3$ on electronic conductivity, the cells were deliberately cycled at 0.2 C rate (1C = 147 mAh g^{-1}) for 3 cycles before carrying out the cycling performances at different current densities. Cyclic voltammetry (CV) was measured at different scan rate ranging from 3.4 to 4.9 V. Electrochemical impedance spectra (EIS) were recorded on electrochemical workstation (CHI660C) with applied 10 mV sinusoidal perturbation in a frequency range from 100 kHz to 10 mHz at room temperature.

3. Results and discussion

3.1. Material characterization

Typical XRD patterns of $LiNi_{0.5}Mn_{1.5}O_4$ and $(LiNi_{0.5}Mn_{1.5}O_4)_{94}/(La_{0.7}Sr_{0.3}MnO_3)_6$ denoted as Samples A and B, are shown in Fig. 1, respectively. Two sets of XRD patterns corresponding to $LiNi_{0.5}Mn_{1.5}O_4$ (ICSD#070046) and $La_{0.7}Sr_{0.3}MnO_3$ (ICSD#050717) phases are observed clearly. There are no Bragg diffraction peaks of third phases within the sensitivity of measurement, indicating that no chemical reaction occurs between two components during the high-temperature calcination.

Fig. 2 (a) and (b) shows the morphologies of pristine $LiNi_{0.5}Mn_{1.5}O_4$ and $La_{0.7}Sr_{0.3}MnO_3$ modified $LiNi_{0.5}Mn_{1.5}O_4$ particles, respectively. A smooth and clean surface was observed on

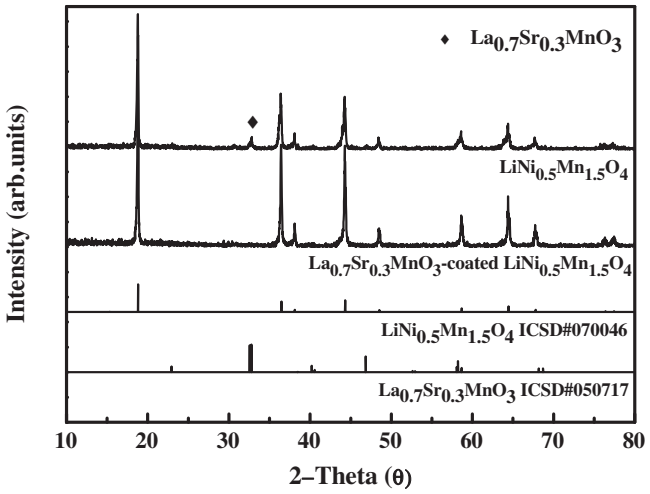

Fig. 1. XRD patterns of (a) the as-prepared $LiNi_{0.5}Mn_{1.5}O_4$ and (b) $La_{0.7}Sr_{0.3}MnO_3$-coated $LiNi_{0.5}Mn_{1.5}O_4$ cathode material.

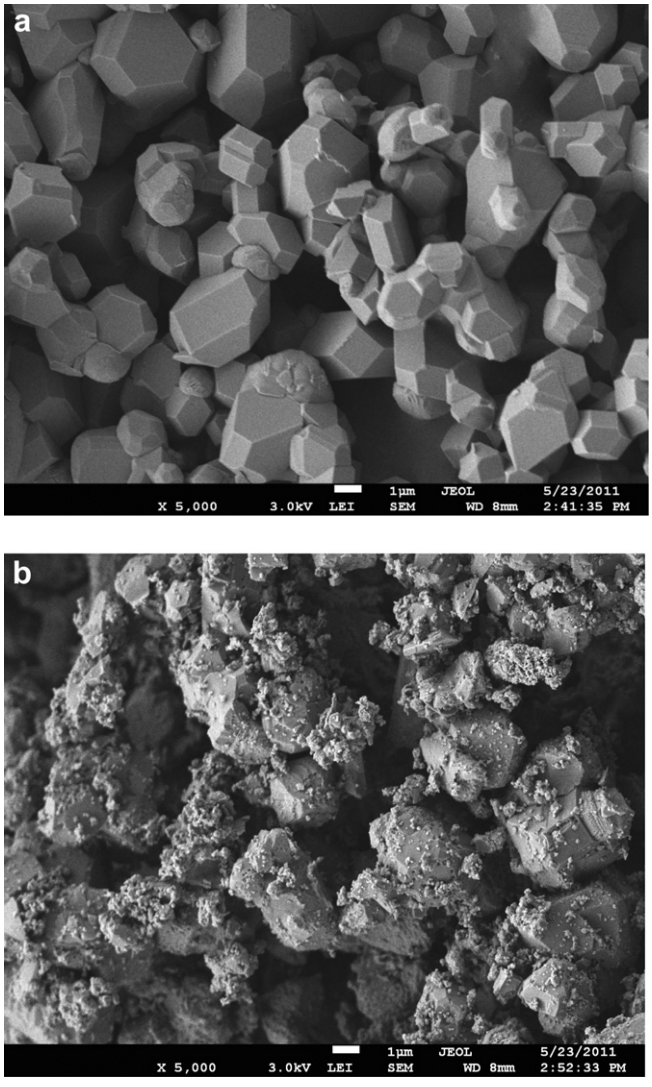

Fig. 2. SEM photographs of (a) the as-prepared $LiNi_{0.5}Mn_{1.5}O_4$ and (b) $La_{0.7}Sr_{0.3}MnO_3$-coated $LiNi_{0.5}Mn_{1.5}O_4$ cathode material.

the $LiNi_{0.5}Mn_{1.5}O_4$ particle (Fig. 2a) and $La_{0.7}Sr_{0.3}MnO_3$ nanoparticles with the order of ~10 nm were found to be uniformly distributed over the surface of $LiNi_{0.5}Mn_{1.5}O_4$ particles, as seen in Fig. 2b.

3.2. Electrochemical properties

Fig. 3(a) shows the typical cyclic performances of the electrodes comprising Samples A and B as the cathode at a current rate of 2C at 25 °C, respectively. The beneficial effect of $La_{0.7}Sr_{0.3}MnO_3$-coating on enhancing electrochemical performances is obviously observed. Although Sample A demonstrates larger capacity than that of Sample B in the initial cycles which is attributed to the electrochemically inactive $La_{0.7}Sr_{0.3}MnO_3$, the capacity retention rates of Sample A and B after 100 cycles are 67% and 91%, respectively. The poor cycling performance of the pristine $LiNi_{0.5}Mn_{1.5}O_4$ results from the high surface reactivity of the Ni^{4+} from the charged cathode with the electrolyte [8]. The $La_{0.7}Sr_{0.3}MnO_3$ coating layer protects the surface of $LiNi_{0.5}Mn_{1.5}O_4$ from HF in the electrolyte during electrochemical cycling. As a result, the dissolution of transition metal elements is suppressed and the electrochemical reversibility is correspondingly improved.

It is well-known that electrode performance depends strongly on the electrode microstructure and morphology besides the nature of cathode material [15]. Fig. 3(b) shows the cycling performances of Sample A and B cathode at different discharge rates (0.5C, 1C, 2C, 3C) between 3.0 and 4.9 V. The Sample B (0.5C: 129 mAh g^{-1}; 1C: 124 mAh g^{-1}; 2C: 118 mAh g^{-1}; 3C: 113 mAh g^{-1}, respectively) exhibits higher discharge capacity than Sample A (0.5C: 116 mAh g^{-1}; 1C: 105 mAh g^{-1}; 2C: 95 mAh g^{-1}; 3C: 80 mAh g^{-1}, respectively). The increment in capacity reveals that the surface modification with $La_{0.7}Sr_{0.3}MnO_3$ does facilitate the electrochemical insertion/extraction process of Li^+ ion even at the high discharge rates.

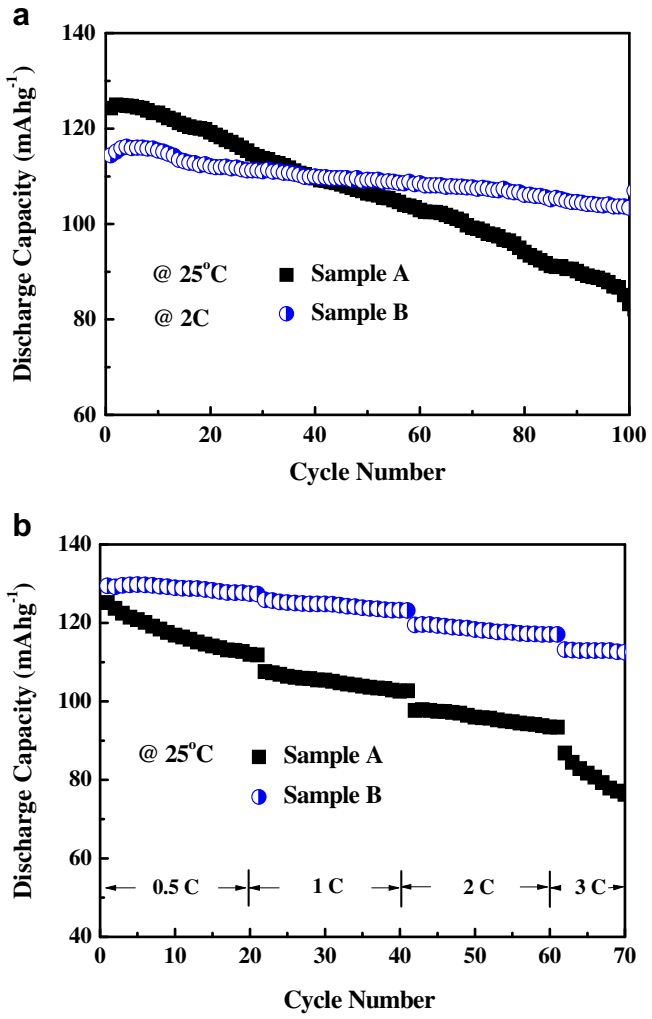

Fig. 3. (a) Cycling behavior at 2C and (b) Rate capabilities of pristine and $La_{0.7}Sr_{0.3}MnO_3$-coated $LiNi_{0.5}Mn_{1.5}O_4$ spinel at 25 °C.

Fig. 4(a) and (b) presents four groups of CV curves of Sample A and Sample B, measured at the sweep rates of 0.03, 0.05, 0.08 and 0.1 mV s^{-1} ranging from 3.0 to 4.9 V, respectively. The observed anodic peaks mainly at 4.05, 4.65 and 4.8 V correspond to the transition of Mn^{3+}/Mn^{4+}, Ni^{2+}/Ni^{3+} and Ni^{3+}/Ni^{4+}, respectively. Fig. 4(c) and (d) shows the relationship between the peak current and the sweep rate, which could be expressed as follows [11]:

$$I_p = 2.69 \times 10^5 n^{3/2} A D^{1/2} C_{Li} v^{1/2} \quad (1)$$

Where I_p is the peak current, n is the number of electron involved in the reaction, A is the active surface area of the electrode, C_{Li} is the concentration of Li^+ ions in the electrode and v is the sweep rate, respectively. Based on Eq. (1), the Li^+ diffusion coefficients (D) of pristine and $La_{0.7}Sr_{0.3}MnO_3$-coated $LiNi_{0.5}Mn_{1.5}O_4$ can be calculated and the corresponding values are listed in Table 1. The data presented in Table 1 clearly demonstrate that the kinetics of Li^+ diffusion is be enhanced by coating high electronic conductivity $La_{0.7}Sr_{0.3}MnO_3$ on $LiNi_{0.5}Mn_{1.5}O_4$ surface due to the enhancement in electronic conductivity, resulting in the superior rate behavior to the $La_{0.7}Sr_{0.3}MnO_3$-coated $LiNi_{0.5}Mn_{1.5}O_4$. On the other hand, it is well-known that LiF, a high impedance for Li-ion transport, would form on the surfaces of cathode materials due to the reaction between carbonate species and HF in the electrolyte. For the battery system with $La_{0.7}Sr_{0.3}MnO_3$-coated sample, the dissolution of Ni or Mn was effectively reduced by the reaction between $La_{0.7}Sr_{0.3}MnO_3$ and HF. As a result, $La_{0.7}Sr_{0.3}MnO_3$-coated $LiNi_{0.5}Mn_{1.5}O_4$ with lower content of LiF exhibits enhanced Li^+ diffusion in comparison with the pristine sample.

To get insight into the reason behind the enhancement of electrochemical performance with $La_{0.7}Sr_{0.3}MnO_3$-coating, the stability of the pristine and $La_{0.7}Sr_{0.3}MnO_3$-coated $LiNi_{0.5}Mn_{1.5}O_4$ at elevated temperature was systematically investigated. The cells of $LiNi_{0.5}Mn_{1.5}O_4$ Vs Li and $La_{0.7}Sr_{0.3}MnO_3$-coated $LiNi_{0.5}Mn_{1.5}O_4$ Vs Li were thermal-annealed at 60 °C for 3 days, denoted as Sample AA and Sample BB respectively. Fig. 5(a) and (b) presents the capacity cyclability of Sample A and B at 2C and 60 °C, Sample AA and BB at 2C and 25 °C, respectively. Compared to $La_{0.7}Sr_{0.3}MnO_3$-coated $LiNi_{0.5}Mn_{1.5}O_4$, the pristine $LiNi_{0.5}Mn_{1.5}O_4$ samples are found to be more pronounced with cycling. The discharge capacities in the 1st and 100th cycles of Sample A are 123 and 50 mAh g^{-1}, respectively, with capacity retention of 41%. The cycling performances of Sample B remarkably improved, which the capacity retention is near to 90% of the initial capacity after 100 cycles, demonstrating the extraordinary cycling stability at elevated temperature. In the case of storage at elevated temperature, the capacity retention of Sample BB is near to 90% of the initial capacity after 100 cycles, suggesting the extraordinary cycling stability at elevated temperature, while Sample AA electrode suffered a more than 50% capacity loss. The pronounced dissolution of transition metal ions at elevated temperature is considered to be responsible for the severe capacity fade of the spinel powder [16]. The dissolved amounts of transition metal elements were analyzed by measured by ICP after the fully charged electrodes were stored in fresh electrolytes at 60 °C for 4 weeks. The dissolved contents of Ni and Mn in electrolyte for the

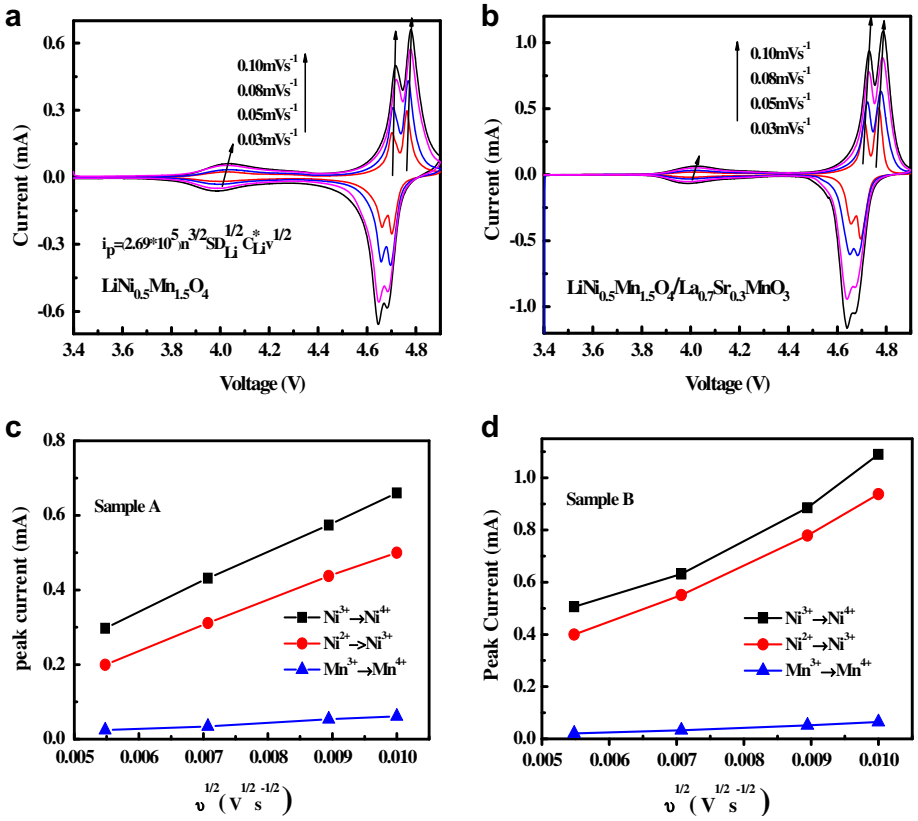

Fig. 4. (a, b) CV curves at a series of sweep rates and (c, d) relationship between the peak current and the square root of sweep rate for pristine and $La_{0.7}Sr_{0.3}MnO_3$-coated $LiNi_{0.5}Mn_{1.5}O_4$ spinel.

pristine $LiNi_{0.5}Mn_{1.5}O_4$ were 65.07 and 181.07 mg L^{-1}, while the $La_{0.7}Sr_{0.3}MnO_3$-coated $LiNi_{0.5}Mn_{1.5}O_4$ demonstrated smaller Ni and Mn dissolutions of 43.21 and 132.26 mg L^{-1}, respectively. The reduced dissolution of transition metals indicate that $La_{0.7}Sr_{0.3}MnO_3$ coating layer coated on the $LiNi_{0.5}Mn_{1.5}O_4$ powder functions as a protective film, which is beneficial to suppress the surface erosion caused by HF in the electrolyte and consequently enhance the cyclic stability of the electrode. On the other hand, Mn dissolution from $La_{0.7}Sr_{0.3}MnO_3$ is expected to also suppress dynamically the erosion of $LiNi_{0.5}Mn_{1.5}O_4$ particles by the electrolyte.

Fig. 6 shows the cycling performances of Sample A and B at different current densities at 60 °C, respectively. The beneficial effect of $La_{0.7}Sr_{0.3}MnO_3$-coating in reducing capacity fading of $LiNi_{0.5}Mn_{1.5}O_4$ at elevated temperature is clearly observed and Sample B (0.5C: 129 mAh g^{-1}; 1C: 120 mAh g^{-1}; 2C: 109 mAh g^{-1}; 3C: 105 mAh g^{-1}, respectively) shows better electrochemical performance than that of Sample A (0.5C: 111 mAh g^{-1}; 1C: 94 mAh g^{-1}; 2C: 83 mAh g^{-1}; 3C: 73 mAh g^{-1}, respectively). The beneficial effect of $La_{0.7}Sr_{0.3}MnO_3$-coating on thermal-storage stability at elevated temperature is investigated by electrochemical impedance spectroscopy measurement.

Table 1
The Li^+ diffusion coefficients (D) of pristine and $La_{0.7}Sr_{0.3}MnO_3$-coated $LiNi_{0.5}Mn_{1.5}O_4$.

Li^+ diffusion coefficients D (cm^2 s^{-1})	Mn^{3+}/Mn^{4+}	Ni^{2+}/Ni^{3+}	Ni^{3+}/Ni^{4+}
Pristine $LiNi_{0.5}Mn_{1.5}O_4$	7×10^{-11}	1.14×10^{-10}	2.05×10^{-10}
$LaSr_{0.3}Mn_{0.7}O_3$-coated $LiNi_{0.5}Mn_{1.5}O_4$	8×10^{-11}	2.02×10^{-10}	3.3×10^{-10}

Fig. 7 presents EIS profiles of Sample A and B after 50 cycles at a 2C rate in 60 °C at the fully discharge state and the corresponding equivalent circuit. According to the literature [8], the symbols, R_e, R_{sf}, R_{ct}, and R_w, represent the solution resistance, the diffusion resistance of Li^+ ions through SEI layer, the charge-transfer resistance and Warburg impedance, respectively. According to the equivalent circuit, individual contribution from each of solution resistance, diffusion resistance and charge-transfer resistance are calculated as 5.724 Ω, 139 Ω and 48.62 Ω for Sample A and 7.889 Ω, 47.61 Ω and 18.57 Ω for Sample B, respectively. Change in solution resistance is small due to electrochemical inactive $La_{0.7}Sr_{0.3}MnO_3$-coating [8] and change in the composition of the electrolyte [17]. Compared to $La_{0.7}Sr_{0.3}MnO_3$-coated $LiNi_{0.5}Mn_{1.5}O_4$, the change in charge-transfer resistance of pristine sample is pronounced because the components of electrolyte would be oxidized and decomposed on the cathode surface to form SEI layer (RCH_2OCO_2Li, LiF, MnF_2, Li_2CO_3 and so on), in which the process is accelerated at high-temperature [18,19]. The SEI layer slows down of the kinetics of these electrodes through the obstruction of the pore upon cycling and consequently increase of charge-transfer resistance during cycling [20]. An integrate network formed by $La_{0.7}Sr_{0.3}MnO_3$ acts a highly conductive nanolayer between particles due to its high electronic conductivity. Based on scattering theory of electron transport across the interface [21], a phenomenological model for charge-transfer resistance in $La_{0.7}Sr_{0.3}MnO_3/LiNi_{0.5}Mn_{1.5}O_4$ composite is set up and a corresponding equivalent circuit of two-parallel diffusion paths describing these processes is presented in Fig. 8, where R_L represents the resistance of $La_{0.7}Sr_{0.3}MnO_3$ and R_E is surface resistance arising from the decomposition of the electrolyte. Due to the high electronic conductivity of $La_{0.7}Sr_{0.3}MnO_3$, the total resistance of two resistors in parallel is much small in

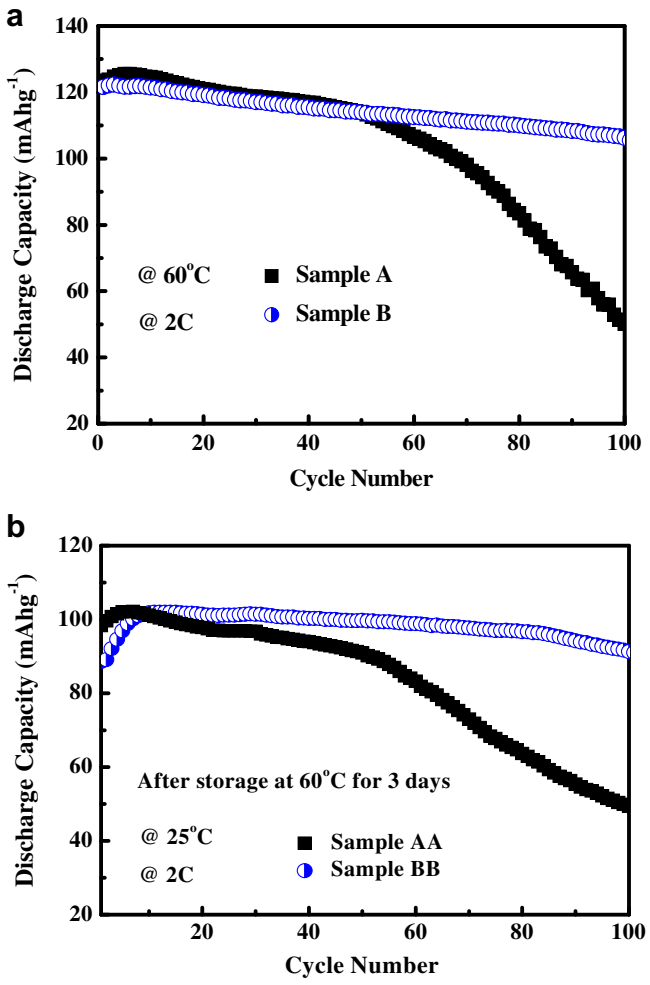

Fig. 5. (a) The discharge capacity versus cycle number for $LiNi_{0.5}Mn_{1.5}O_4$ (denoted as Sample A) and $La_{0.7}Sr_{0.3}MnO_3$-coated $LiNi_{0.5}Mn_{1.5}O_4$ (denoted as Sample B) at 2C and 60 °C; (b) Room temperature cycling performances of $LiNi_{0.5}Mn_{1.5}O_4$ and $La_{0.7}Sr_{0.3}MnO_3$-coated $LiNi_{0.5}Mn_{1.5}O_4$ thermal-annealed at 60 °C for 3 days at 2C, denoted as Sample AA and Sample BB respectively.

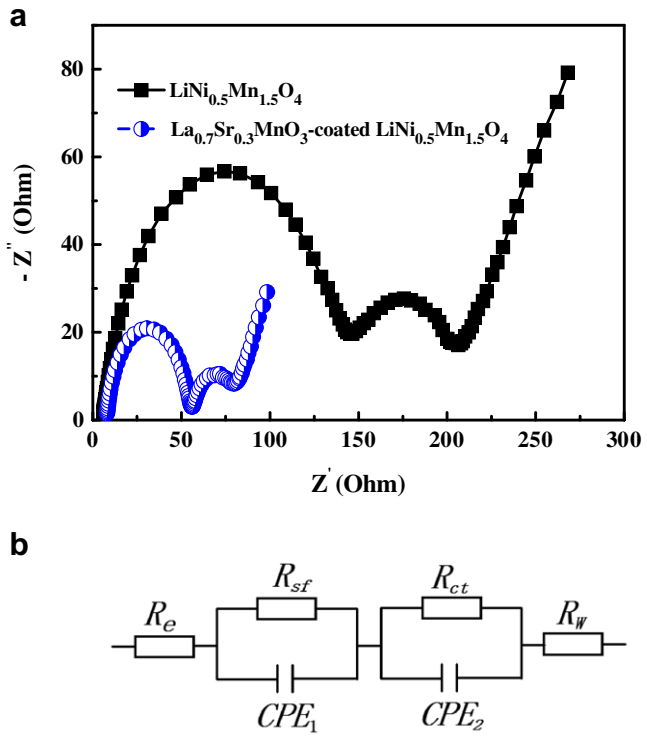

Fig. 7. (a) The EIS profiles of $LiNi_{0.5}Mn_{1.5}O_4$ (denoted as Sample A) and $La_{0.7}Sr_{0.3}MnO_3$-coated $LiNi_{0.5}Mn_{1.5}O_4$ (denoted as Sample B) after 50 cycles at a 2C rate in 60 °C at the fully discharge state; (b) the equivalent circuit for EIS results fitting.

comparison with the pristine one. Thus, the existence of high conductive $La_{0.7}Sr_{0.3}MnO_3$ on the surface of the cathode is beneficial to reduce the charge-transfer resistance and overall polarization resistance. In addition, the presence of $La_{0.7}Sr_{0.3}MnO_3$ on $LiNi_{0.5}Mn_{1.5}O_4$ particles is expected to suppress the occurrence of undesirable side-reactions between the electrolyte and electrode at high voltage and high-temperature, and consequently decrease the SEI and charge-transfer resistances. As a result, the cycling stability is improved with $La_{0.7}Sr_{0.3}MnO_3$-coating, especially at elevated temperature.

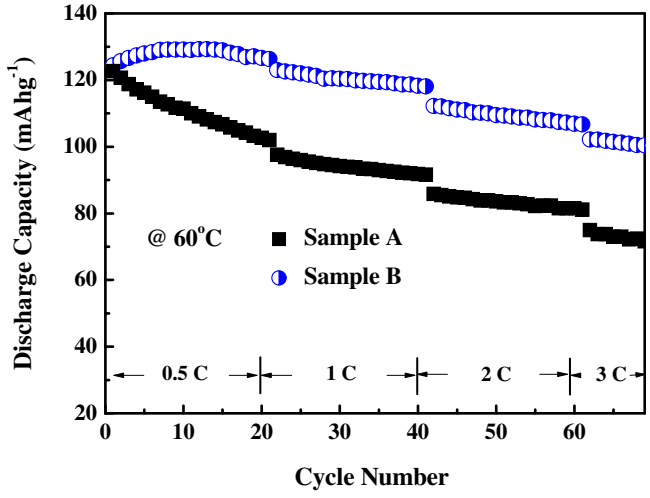

Fig. 6. Cycling performances of $LiNi_{0.5}Mn_{1.5}O_4$ (denoted as Sample A) and $La_{0.7}Sr_{0.3}MnO_3$-coated $LiNi_{0.5}Mn_{1.5}O_4$ (denoted as Sample B) at different current densities at 60 °C.

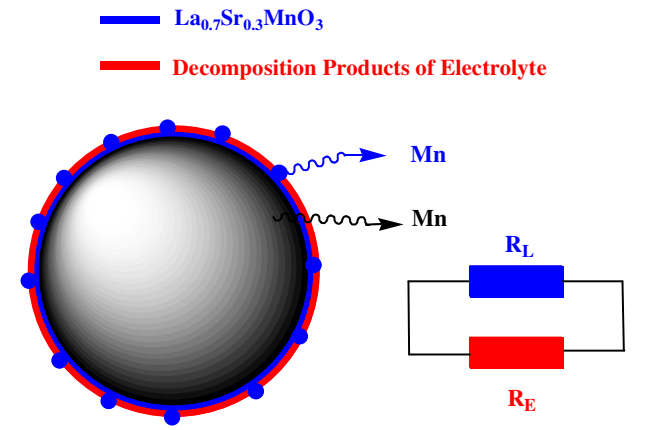

Fig. 8. Phenomenological model for charge-transfer resistance in $La_{0.7}Sr_{0.3}MnO_3$-coated $LiNi_{0.5}Mn_{1.5}O_4$ composite and a corresponding equivalent circuit of two-parallel diffusion paths. The Li^+ diffusion coefficients (D) of pristine and $La_{0.7}Sr_{0.3}MnO_3$-coated $LiNi_{0.5}Mn_{1.5}O_4$.

4. Conclusion

Pristine and $La_{0.7}Sr_{0.3}MnO_3$-coated $LiNi_{0.5}Mn_{1.5}O_4$ cathode materials were prepared by a sol–gel method. Compared to the pristine $LiNi_{0.5}Mn_{1.5}O_4$, $La_{0.7}Sr_{0.3}MnO_3$-coated $LiNi_{0.5}Mn_{1.5}O_4$ has a better cycle stability and rate performance, especially at elevated temperature. The presence of $La_{0.7}Sr_{0.3}MnO_3$-coated-layer on $LiNi_{0.5}Mn_{1.5}O_4$ surface is considered to play a positive role in suppressing the dissolution of Mn from the spinel material and improving electronic conductivity, resulting in reducing capacity fading and enhancing high C rate performances.

Acknowledgements

This work was supported by a grant from National Science Foundation for Young Scholars (No. 11004032), Natural Science Foundation of China (No. 11074039) and the National Key Project for Basic Research of China (No. 2011CBA00200).

References

[1] R. Santhanam, B. Rambabu, J. Power Sources 195 (2010) 5442.
[2] S. Patoux, L. Daniel, C. Bourbon, H. Lignier, C. Pagano, F. Le Cras, S. Jouanneau, S. Martinet, J. Power Sources 189 (2009) 344.
[3] M. Kunduraci, J.F. Al-Sharab, G.G. Amatucci, Chem. Mater. 18 (2006) 3585.
[4] Y.K. Sun, C.S. Yoon, I.H. Oh, Electrochim. Acta 48 (2003) 503.
[5] J.C. Arrebola, A. Caballero, L. Hernán, J. Morales, J. Power Sources 195 (2010) 4278.
[6] Y.K. Fan, J.M. Wang, Z. Tang, W.C. He, J.Q. Zhang, Electrochim. Acta 52 (2007) 3870.
[7] J.Y. Shi, C.W. Yic, K. Kim, J. Power Sources 195 (2010) 6860.
[8] H.M. Wu, I. Belharouak, A. Abouimrane, Y.-K. Sun, K. Amine, J. Power Sources 195 (2010) 2909.
[9] H.B. Kang, S.T. Myung, K. Amine, S.M. Lee, Y.K. Sun, J. Power Sources 195 (2010) 2023.
[10] R.S. Guo, Q.T. Wei, H.L. Li, F.H. Wang, Mater. Lett. 60 (2006) 261.
[11] T.Y. Yang, N.Q. Zhang, L.G. Ye, K.N. Sun, Electrochim. Acta 56 (2011) 4058.
[12] C. Li, H.P. Zhang, L.J. Fu, H. Liu, Y.P. Wu, E. Rahm, R. Holze, H.Q. Wu, Electrochim. Acta 51 (2006) 3872.
[13] Y. Cui, X.L. Zhao, R.S. Guo, Electrochim. Acta 55 (2010) 922.
[14] Y.B. Lin, Z.G. Huang, Y.M. Yang, S. Wang, S.D. Li, F.M. Zhang, Y.W. Du, Appl. Phys. A 104 (2011) 143.
[15] J.W. Fergus, J. Power Sources 195 (2010) 939.
[16] D. Aurbach, B. Markovsky, Y. Talyossef, G. Salitra, H.-J. Kim, S.D. Choi, J. Power Sources 162 (2006) 780.
[17] D. Aurbach, A. Schechter, Electrochem. Acta 46 (2001) 2395.
[18] K. Xu, Chem. Rev. 104 (2004) 4303.
[19] B.J. Hwanga, Y.W. Wu, M. Venkateswarlu, M.Y. Cheng, R. Santhanam, J. Power Sources 193 (2009) 828.
[20] B. Markovsky, Y. Talyossef, G. Salitra, D. Aurbach, H.-J. Kim, S. Choi, Electrochem. Commun. 6 (2004) 821.
[21] Z.G. Huang, Z.G. Chen, K. Peng, D.H. Wang, F.M. Zhang, W.Y. Zhang, Y.W. Du, Phys. Rev. B 69 (2004) 094420.